Supporting information

Integrated Platform for Expedited Synthesis-Purification-Testing of Small Molecule Libraries.

Aleksandra Baranczak[a†], Noah P. Tu[a†], Jasmina Marjanovic[a], Philip A. Searle[a], Anil Vasudevan[a]*, Stevan W. Djuric[a]

[a] Discovery Chemistry and Technology, AbbVie Inc., 1 North Waukegan Rd., North Chicago, IL 60064

Table of Contents

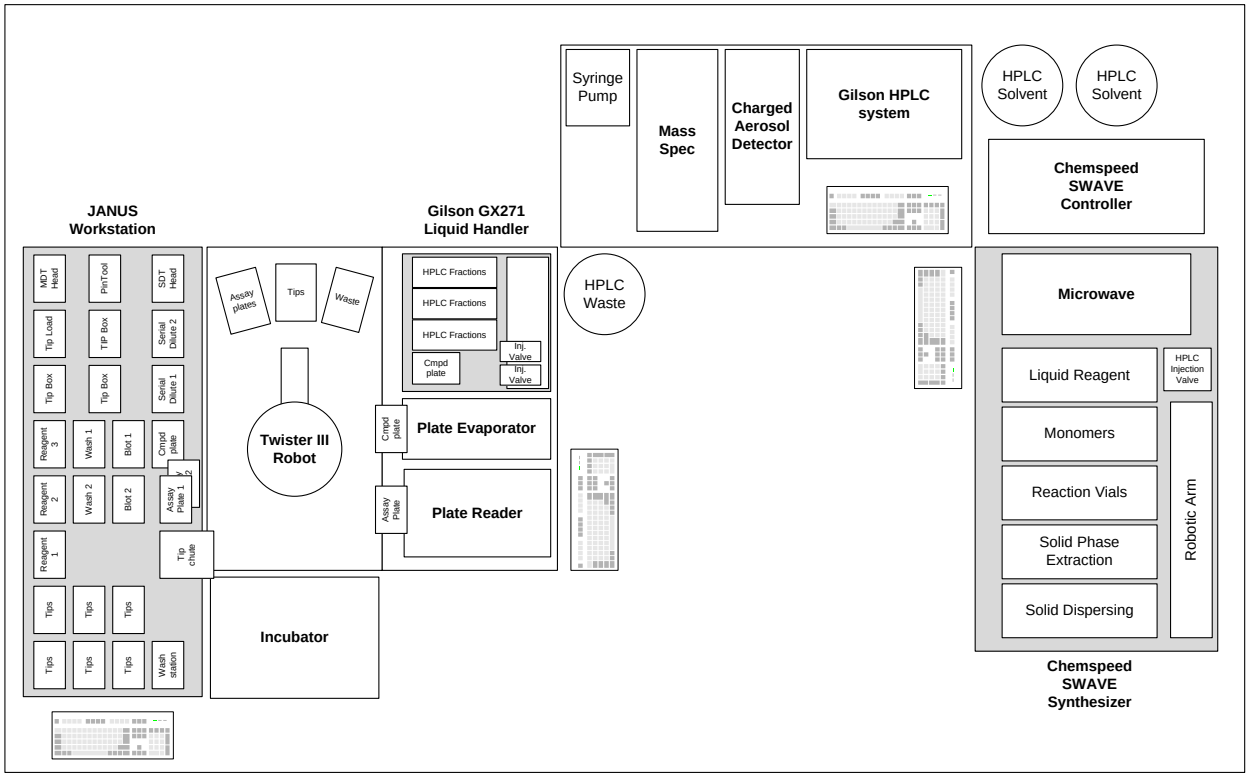

Figure S1. Schematic representation of integrated synthesis-purification-bioassay platform.

A

	1	2	3	4	5	6	7	8	9	10	11	12
A	1	9	17	25	33	41	1	9	17	25	33	41
B	2	10	18	26	34	42	2	10	18	26	34	42
C	3	11	19	27	35	43	3	11	19	27	35	43
D	4	12	20	28	36	44	4	12	20	28	36	44
E	5	13	21	29	37	45	5	13	21	29	37	45
F	6	14	22	30	38	46	6	14	22	30	38	46
G	7	15	23	31	39	47	7	15	23	31	39	47
H	8	16	24	32	40	48	8	16	24	32	40	48

B

	1	2	3	4	5	6	7	8	9	10	11	12
A	Control	5	13	21	29	37	1	9	17	25	33	41
B	Control	6	14	22	30	38	2	10	18	26	34	42
C	Control	7	15	23	31	39	3	11	19	27	35	43
D	Control	8	16	24	32	40	4	12	20	28	36	44
E	1	9	17	25	33	41	5	13	21	29	37	
F	2	10	18	26	34	42	6	14	22	30	38	
G	3	11	19	27	35	43	7	15	23	31	39	
H	4	12	20	28	36	44	8	16	24	32	40	

C

	1	2	3	4	5	6	7	8	9	10	11	12	13	14	15	16	17	18	19	20	21	22	23	24
A	10	3.3	1.1	0.37	0.12	0.041	0.014	4.6E-03	1.5E-03	5.1E-04	1.7E-04	10.0	3.3	1.1	0.37	0.12	0.041	0.014	4.6E-03	1.5E-03	5.1E-04	1.7E-04	Control	Control
B	10	3.3	1.1	0.37	0.12	0.041	0.014	4.6E-03	1.5E-03	5.1E-04	1.7E-04	10.0	3.3	1.1	0.37	0.12	0.041	0.014	4.6E-03	1.5E-03	5.1E-04	1.7E-04	Control	Control
C	10	3.3	1.1	0.37	0.12	0.041	0.014	4.6E-03	1.5E-03	5.1E-04	1.7E-04	10.0	3.3	1.1	0.37	0.12	0.041	0.014	4.6E-03	1.5E-03	5.1E-04	1.7E-04	Control	Control
D	10	3.3	1.1	0.37	0.12	0.041	0.014	4.6E-03	1.5E-03	5.1E-04	1.7E-04	10.0	3.3	1.1	0.37	0.12	0.041	0.014	4.6E-03	1.5E-03	5.1E-04	1.7E-04	Control	Control
E	10	3.3	1.1	0.37	0.12	0.041	0.014	4.6E-03	1.5E-03	5.1E-04	1.7E-04	10.0	3.3	1.1	0.37	0.12	0.041	0.014	4.6E-03	1.5E-03	5.1E-04	1.7E-04	Control	Control
F	10	3.3	1.1	0.37	0.12	0.041	0.014	4.6E-03	1.5E-03	5.1E-04	1.7E-04	10.0	3.3	1.1	0.37	0.12	0.041	0.014	4.6E-03	1.5E-03	5.1E-04	1.7E-04	Control	Control
G	10	3.3	1.1	0.37	0.12	0.041	0.014	4.6E-03	1.5E-03	5.1E-04	1.7E-04	10.0	3.3	1.1	0.37	0.12	0.041	0.014	4.6E-03	1.5E-03	5.1E-04	1.7E-04	Control	Control
H	10	3.3	1.1	0.37	0.12	0.041	0.014	4.6E-03	1.5E-03	5.1E-04	1.7E-04	10.0	3.3	1.1	0.37	0.12	0.041	0.014	4.6E-03	1.5E-03	5.1E-04	1.7E-04	Control	Control
I	10	3.3	1.1	0.37	0.12	0.041	0.014	4.6E-03	1.5E-03	5.1E-04	1.7E-04	10.0	3.3	1.1	0.37	0.12	0.041	0.014	4.6E-03	1.5E-03	5.1E-04	1.7E-04	Control	Control
J	10	3.3	1.1	0.37	0.12	0.041	0.014	4.6E-03	1.5E-03	5.1E-04	1.7E-04	10.0	3.3	1.1	0.37	0.12	0.041	0.014	4.6E-03	1.5E-03	5.1E-04	1.7E-04	Control	Control
K	10	3.3	1.1	0.37	0.12	0.041	0.014	4.6E-03	1.5E-03	5.1E-04	1.7E-04	10.0	3.3	1.1	0.37	0.12	0.041	0.014	4.6E-03	1.5E-03	5.1E-04	1.7E-04	Control	Control
L	10	3.3	1.1	0.37	0.12	0.041	0.014	4.6E-03	1.5E-03	5.1E-04	1.7E-04	10.0	3.3	1.1	0.37	0.12	0.041	0.014	4.6E-03	1.5E-03	5.1E-04	1.7E-04	Control	Control
M	10	3.3	1.1	0.37	0.12	0.041	0.014	4.6E-03	1.5E-03	5.1E-04	1.7E-04	10.0	3.3	1.1	0.37	0.12	0.041	0.014	4.6E-03	1.5E-03	5.1E-04	1.7E-04	Control	Control
N	10	3.3	1.1	0.37	0.12	0.041	0.014	4.6E-03	1.5E-03	5.1E-04	1.7E-04	10.0	3.3	1.1	0.37	0.12	0.041	0.014	4.6E-03	1.5E-03	5.1E-04	1.7E-04	Control	Control
O	10	3.3	1.1	0.37	0.12	0.041	0.014	4.6E-03	1.5E-03	5.1E-04	1.7E-04	10.0	3.3	1.1	0.37	0.12	0.041	0.014	4.6E-03	1.5E-03	5.1E-04	1.7E-04	Control	Control
P	10	3.3	1.1	0.37	0.12	0.041	0.014	4.6E-03	1.5E-03	5.1E-04	1.7E-04	10.0	3.3	1.1	0.37	0.12	0.041	0.014	4.6E-03	1.5E-03	5.1E-04	1.7E-04	Control	Control

Figure S2. Schematic representation of 96-well and 384-deep well plate arrangement.

A. Arrangement of 96-well plate for 48-member library. Sample aliquots for bioassay are collected in wells A1-H6. Sample aliquots for NMR analysis are collected in wells A7-H12.

B. Arrangement of 96-well plate for 44-member library with inclusion of four reference compounds for bioassay. Sample aliquots for bioassay are collected in wells E1-H6. Sample aliquots for NMR analysis are collected in wells A7-D12.

C. Arrangement of 384-deep well plate for 11-point, 3-fold serial dilution. Total of 32 compounds undergo serial dilution in one 384-deep well plate. Wells in columns 23 and 24 are devoted to control buffer solutions: DMSO only (positive control, column 23), no protein (negative control, column 24).

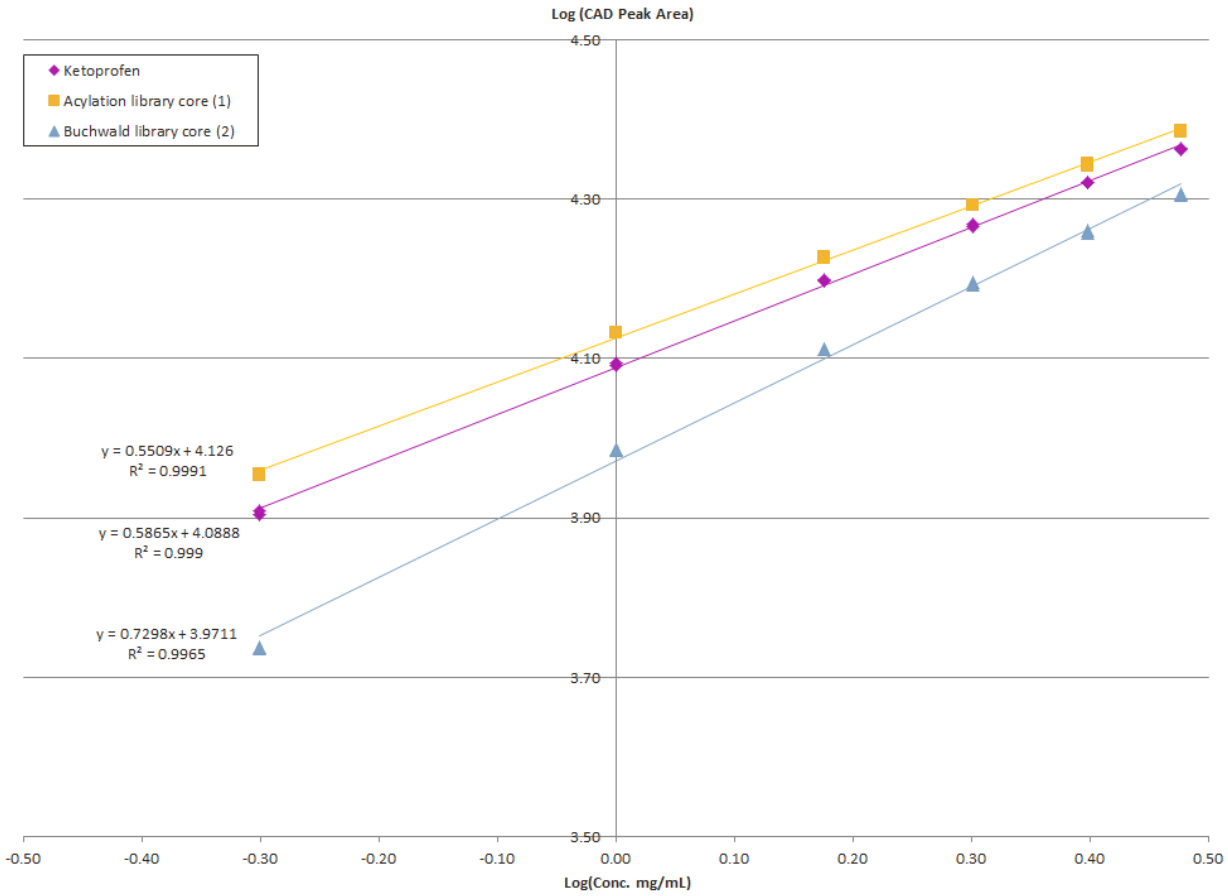

Figure S3. Comparison of CAD response for ketoprofen and library core materials, compounds **1** and **2**.

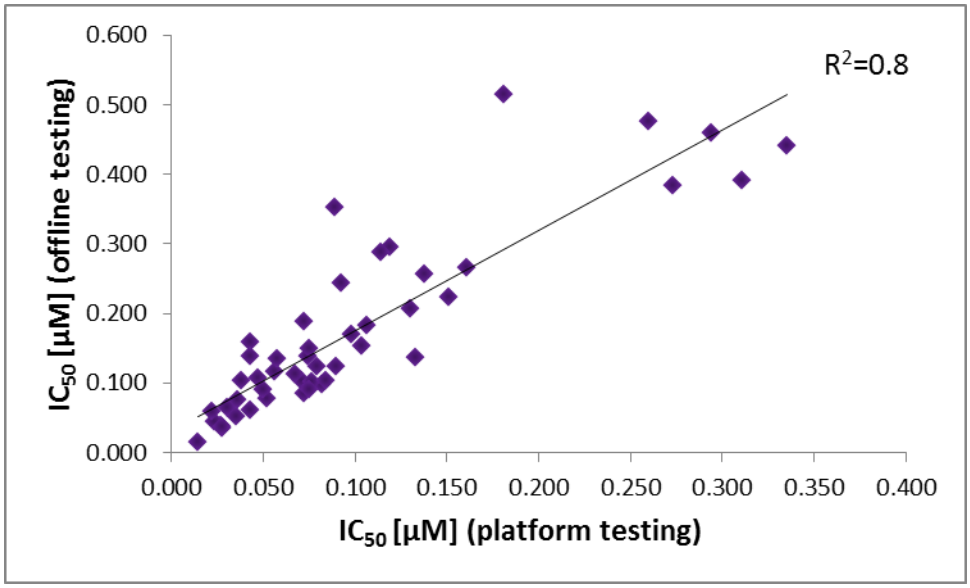

Figure S4. Correlation between platform data (platform testing) and data generated through a conventional approach (offline testing).

General information

The synthesis portion of the integrated system employed the commercially available Chemspeed SWAVE [1] synthesizer capable of assembling and delivering both solid and liquid reagents to reaction container. The preparative HPLC-MS purification system was developed in-house using components from several vendors and was integrated with the synthesizer as described previously[2] with the addition of a Corona® CAD® detector from Thermo Scientific.[3] Solvent, chemicals and bioassay reagents were purchased from commercial sources and used directly without further purification. ^{1}H NMR spectra were recorded with Agilent 400-MR, Varian Inova 500 MHz, Varian VNMRS 500 MHz, Bruker Avance III 500 MHz. Chemical shifts were reported in ppm using either TMS or deuterated solvents as internal standards (TMS, 0.00; $CDCl_3$, 7.26; CD_3OD, 3.34; DMSO-d_6, 2.50). Multiplicity was reported as follows: s = singlet, d = doublet, t = triplet, q = quartet, p = pentet, m = multiplet, brs = broad.

HPLC-MS System

The HPLC system consisted of the following components: Gilson 305 and 306 HPLC pumps with 50 mL pump heads; Gilson 806 manometric module; Gilson 155 UV/VIS detector with preparative flow cell (0.05 mm path length, 0.7 µL volume); Gilson GX271 liquid handler for fraction collection with three code 22 racks for 18 × 150 mm test tubes for a total capacity 132 tubes; and Gilson 506C Interface box for digital I/O communication with the SWAVE system and acquisition of analog UV signals from the UV detector. The system was plumbed in a 2-pump 'at-column dilution' configuration[4] with the organic phase pump plumbed through the Valco injection valve (W Type, 5 mL sample loop), and then the stream mixed with the flow from the aqueous phase pump via a mixing tee immediately prior to the HPLC guard column. Typical injection volumes ranged from 1 mL to 3.5 mL. The MS system consisted of a Thermo Scientific™ MSQ-Plus™ single quadrupole mass spectrometer operating in APCI mode: probe temperature 550 ºC; cone voltage 30 V; scan time 0.5 s; and mass range of 170 – 1300 amu. A 4000:1 split of the stream from the preparative HPLC flow was achieved using an Agilent G1968D active splitter and delivered to the MS using a Gilson 305 HPLC pump with 5 mL pump head, operating at 1 mL/min. A mixture of methanol:water (7:3) with 0.1% formic acid was used as the make-up solvent.

The column used was a Phenomenex Luna C8(2), 5 µm, 100Å, 50 × 30 mm, with a SecurityGuard 15 × 30 mm guard column. A typical HPLC method used a gradient of acetonitrile (A) and 0.1%

trifluoroacetic acid in water (B), at a flow rate of 40 mL/min (0 - 1.5 min 3% A, 1.5 – 11.5 min linear gradient 3 - 100% A, 11.5 – 14.0 min 100% A, 14.0 - 16.0 min linear gradient 100 - 3% A). Column equilibration time was dependent upon reaction time but was a minimum of 2 min.

The HPLC-MS system was controlled through a combination of Thermo Scientific Xcalibur™ 2.0.7 software and a custom application written in-house using Microsoft Visual Basic 6.0. The Xcalibur™ software was used for MS method creation and MS data acquisition. The custom application used the Xcalibur™ developers kit (XDK) to send sample sequences to Xcalibur™, initiate data acquisition, and read MS data in real-time. National Instruments Measurement Studio controls were also used for displaying chromatograms. All HPLC components were controlled by the custom application using Gilson serial I/O commands (GSIOC). Communication between HPLC components, the MS and the Chemspeed SWAVE system, was made through digital I/O signals from the Gilson 506C interface box. A purification data browser application was similarly written in Visual Basic 6.0 and used the XDK and National Instruments Measurement Studio controls for displaying chromatograms and mass spectra.

HPLC-MS-CAD integration and measurement of the amount of synthesized compounds

The concentration of purified compounds in HPLC fractions was determined through flow-injection analysis (FIA) of an aliquot of each fraction of interest. To ensure homogeneity of the HPLC fraction, a “bubble-mixing” step was introduced by dispensing air via the injection probe at the bottom of the HPLC fraction. A second injection valve was added to the autosampler/fraction collector of the HPLC system and using an additional analytical HPLC pump, the aliquot was injected into the charged aerosol detector. Using FIA largely eliminates effects due to the solvent composition of the HPLC fraction since the injection volume (20 µL) is negligible compared to the CAD peak volume. The control software automatically determined the fraction of interest for each sample purified, based on the mass spectrometer (MS) signal for the EIC (extracted ion chromatogram) of the target mass for each fraction(s) collected. After injection and acquisition of CAD signal, the software calculated the mass concentration and controlled the autosampler to dispense a specific amount to the compound plate subsequently used for bioassay. The calculation was based upon previous calibration experiments performed using a known control compound (ketoprofen) to determine a Log-Log plot response curve (Figure S3).

Experimental Procedures and Characterization Data

General Library Set-up Procedure

Substrates, amine coupling partners and reaction reagents (in either 4 mL or 40 mL vials) were dissolved in indicated solvents. Solid reagents were pre-mixed inside a glove box. All materials were placed inside the Chemspeed SWAVE system prior to beginning of synthesis. AutoSuite software was used to control assembly of reaction mixtures according to specific reaction conditions (described below). The reaction mixtures were heated using integrated heat strips placed at the bottom of the plate holder with temperature being controlled independently by a digital temperature controller. The countdown timer switch (Traceable Countdown Controller, Part Number 5095) was used to control the heating time. A corresponding wait time was programmed into AutoSuite experiment protocol to account for the time required to complete the heat-strip heating step before subsequent SPE workup/HPLC injection.

Sample lists for the HPLC-UV-MS were created with targeted molecular weight (MW) data exported from an external laboratory information management system (LIMS) as comma-separated variable text files. These MW data and various UV/MS threshold settings were used to customize the purification and collection method for each compound generated from the Chemspeed SWAVE synthesizer.

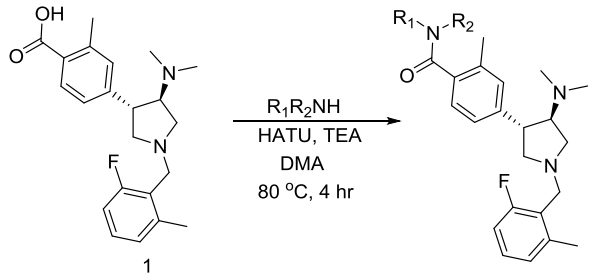

The following stock reagents were prepared and placed on deck of the synthesizer.

1) 4-((3S,4R)-4-(dimethylamino)-1-(2-fluoro-6-methylbenzyl)pyrrolidin-3-yl)-2-methylbenzoic acid (**1**) (536 mg, 1.45 mmol) in DMA (15 mL),
2) 25 amine coupling partners (0.6 mmol, Aldrich Market Select) in DMA (2 mL)
3) Triethylamine (10 mL, Sigma Aldrich, CAS: 121-44-8)
4) HATU (660 mg, 1.73mmol, Sigma Aldrich, CAS: 148893-10-1) in DMA (15mL)

The solution of 4-((3S,4R)-4-(dimethylamino)-1-(2-fluoro-6-methylbenzyl)pyrrolidin-3-yl)-2-methylbenzoic acid (20mg, 0.05 mmol) in DMA (560 µL), amine coupling partner (0.065 mmol) in DMA (216 µL), triethylamine (0.15 mmol, 23 µL), and HATU (0.065 mmol) in DMA (560 µL) were added to 4mL vial equipped with a stir bar and an open top cap with a 13mm PTFE-faced styrene-butadiene rubber cap. The reaction mixtures were heated at 80 °C. After 4 h, the content of each 4mL vial was aspirated and injected into the HPLC injector for purification.

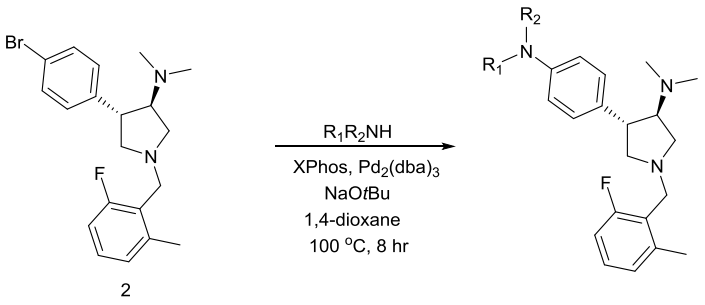

2

(3R,4S)-4-(4-bromophenyl)-1-(2-fluoro-6-methylbenzyl)-N,N-dimethylpyrrolidin-3-amine (**2**) (1000 mg, 2.56 mmol) was dissolved in 1,4-dioxane (35 mL) under inert atmosphere and the vial was sealed. A powder mixture of XPhos (244 mg, Sigma Aldrich, CAS: 564483-18-7), $Pd_2(dba)_3$ (234 mg, Sigma Aldrich, CAS:51364-51-3) and Na*t*OBu (368 mg, Aldrich, CAS:865-48-5) was placed inside the solid dispensing vial. House nitrogen gas (20 psi, 10 GPM) was allowed to fill the chamber of Chemspeed synthesizer for 20 minutes. The solid mixture (XPhos (6.1 mg 0.012 mmol), $Pd_2(dba)_3$ (5.85 mg 0.006 mmol) and NaO*t*Bu (9.21 mg, 0.96 mmol)) was added via a solid dispensing unit to a 4mL vial containing amine coupling partner (0.1 mmol, Aldrich Market Select) and a stir bar. The vials were sealed using an open top cap with a 13mm PTFE-faced styrene-butadiene rubber cap. The solution of bromide **2** (0.875 mL, 0.06 mmol) in 1,4-dioxane (875 µL) was added. The suspension was heated to 100 °C. After 8 h, reaction mixtures were aspirated from 4mL vials and transferred to the solid phase extraction station and the crude reaction mixtures were passed through cartridges containing silica gel/diatomaceous earth (20:80/w:w). The collected filtrates were injected into the HPLC injector for purification.

EED TR-FRET binding assay

A modified TR-FRET LanthaScreen competition assay was utilized to establish the *in vitro* potency of EED inhibitors.[5,6] The binding assay was initiated by adding 50 nL of DMSO compound solution (via Pin Tool) to a 10 µL mixture of GST-tagged EED (1 nM), pyrrolidine inhibitor-based Oregon green (488) probe (400 nM), and terbium-labeled anti-GST antibody (1 nM) in Tris-HCl (20 mM, pH 7.5),

NaCl (200 mM), Tween-20 (0.01%), DTT (1 mM), and BSA (0.05%) (DTT and BSA were added prior to assay initialization) in 384-well Proxy plate. The assay plate was then incubated for 1 hour (25 °C, 98% humidity). After 1 h, the results of the assay were detected on the PerkinElmer EnVision plate reader using a LanthaScreen TR-FRET protocol. The fluorescent signal of the donor was generated by laser excitation of the terbium labeled anti-GST antibody at 337nm. The fluorescence signal of the acceptor probe was measured as a ratio of the signal at 495nm/520nm. The IC_{50} values for each compound were calculated by non-linear regression using a four-parameter logistic equation. The calculations were conducted by fitting normalized data (the data was normalized to percent inhibition by setting the average signal of DMSO only wells to 0% inhibition and no protein control wells to 100% inhibition, Figure S2C) in Assay Explorer.

Table 1, Entry 1

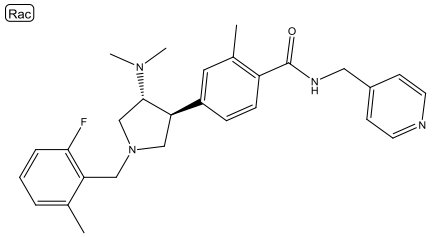

^{1}H NMR (400 MHz, Pyridine-d_5) δ 8.85 (s, 1H), 7.58 (d, *J* = 7.8 Hz, 1H), 7.38 (d, *J* = 5.2 Hz, 2H), 7.29 (d, *J* = 1.7 Hz, 1H), 7.22 (dd, *J* = 7.8, 1.8 Hz, 1H), 7.14 – 7.08 (m, 1H), 6.98 – 6.87 (m, 2H), 4.75 (d, *J* = 5.9 Hz, 2H), 3.69 (d, *J* = 2.3 Hz, 2H), 3.62 – 3.47 (m, 2H), 3.14 – 3.07 (m, 1H), 3.07 – 2.99 (m, 2H), 2.62 – 2.57 (m, 1H), 2.55 (s, 3H), 2.46 (d, *J* = 1.1 Hz, 6H), 2.43 – 2.39 (m, 4H). LRMS (ESI(+)) calcd for $C_{28}H_{33}FN_4O$ $(M+H)^+$ 461.59, found 461.1.

Table 1, Entry 2

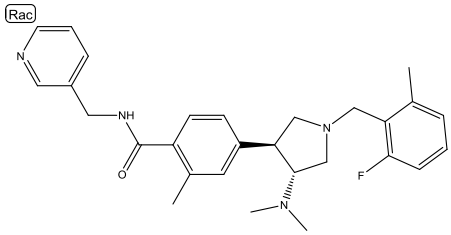

^{1}H NMR (400 MHz, Pyridine-d_5) δ 8.87 (s, 1H), 8.76 (s, 1H), 8.58 (d, *J* = 4.8 Hz, 1H), 7.79 (d, *J* = 7.8 Hz, 1H), 7.26 (s, 1H), 7.22 – 7.17 (m, 2H), 7.12 – 7.07 (m, 1H), 7.00 – 6.86 (m, 2H), 4.75 (d, *J* = 5.8 Hz, 2H), 3.68 (d, *J* = 2.4 Hz, 2H), 3.49 – 3.35 (m, 2H), 3.12 – 2.90 (m, 3H), 2.63 –

2.55 (m, 1H), 2.42 (s, 6H), 2.37 (s, 6H). LRMS (ESI(+)) calcd for $C_{28}H_{33}FN_4O$ $(M+H)^+$ 461.59, found 461.0.

Table 1, Entry 3

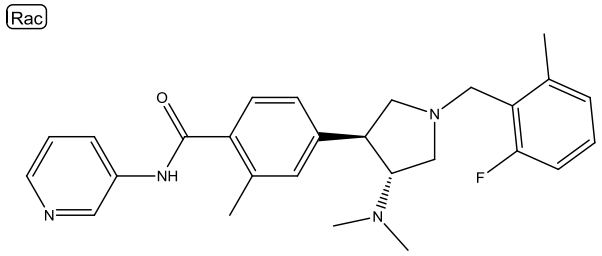

^{1}H NMR (400 MHz, Pyridine-d_5) δ 10.66 (s, 1H), 9.23 (s, 1H), 8.51 – 8.35 (m, 2H), 7.59 – 7.54 (m, 1H), 7.29 – 7.22 (m, 2H), 7.20 – 7.16 (m, 1H), 7.03 – 6.87 (m, 2H), 3.69 (d, *J* = 2.2 Hz, 2H), 3.43 (t, *J* = 5.3 Hz, 2H), 3.16 – 2.88 (m, 3H), 2.63 – 2.54 (m, 1H), 2.52 (s, 3H), 2.42 (d, *J* = 1.8 Hz, 6H), 2.39 (s, 5H). LRMS (ESI(+)) calcd for $C_{27}H_{31}FN_4O$ $(M+H)^+$ 447.56, found 447.1.

Table 1, Entry 4

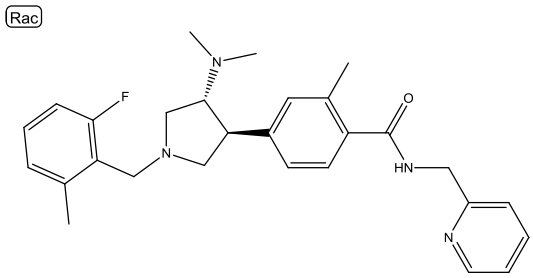

^{1}H NMR (400 MHz, Pyridine-d_5) δ 8.60 – 8.52 (m, 1H), 7.64 – 7.54 (m, 3H), 7.48 – 7.39 (m, 1H), 7.32 – 7.24 (m, 1H), 7.24 – 7.17 (m, 1H), 7.11 – 7.03 (m, 1H), 7.00 – 6.86 (m, 2H), 4.94 (d, *J* = 5.5 Hz, 2H), 3.69 (d, *J* = 2.4 Hz, 2H), 3.54 – 3.41 (m, 2H), 3.16 – 3.04 (m, 1H), 3.04 – 2.95 (m, 2H), 2.64 – 2.55 (m, 3H), 2.47 – 2.34 (m, 12H). LRMS (ESI(+)) calcd for $C_{28}H_{33}FN_4O$ $(M+H)^+$ 461.59, found 461.1.

Table 1, Entry 5

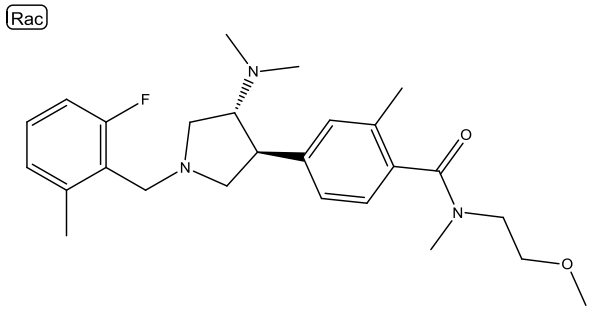

^{1}H NMR (400 MHz, Pyridine-d_5) δ 7.30 (s, 1H), 7.24 (s, 2H), 7.13 – 7.05 (m, 1H), 6.98 – 6.87 (m, 2H), 3.69 (d, *J* = 2.2 Hz, 3H), 3.58 – 3.48 (m, 1H), 3.47 – 3.35 (m, 3H), 3.22 (s, 3H), 3.08 (t, *J* = 8.2 Hz, 1H), 3.03 –

2.87 (m, 3H), 2.85-2.69 (m, 1H), 2.67 – 2.57 (m, 1H), 2.46 – 2.38 (m, 5H), 2.38 – 2.28 (m, 9H). LRMS (ESI(+)) calcd for $C_{26}H_{36}FN_3O_2$ $(M+H)^+$ 442.58, found 442.1.

Table 1, Entry 6

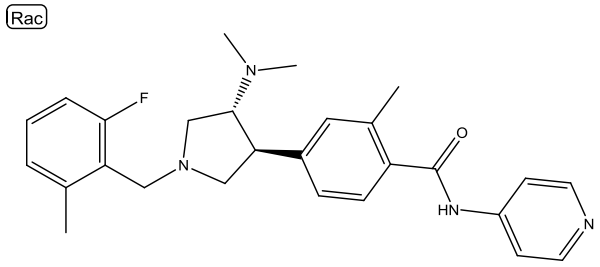

^{1}H NMR (400 MHz, Pyridine-d_5) δ 10.82 (s, 1H), 8.68 – 8.66 (m, 2H), 7.91 (d, *J* = 5.5 Hz, 2H), 7.24 (s, 1H), 7.18 – 7.14 (m, 3H), 7.02 – 6.86 (m, 2H), 3.69 (d, *J* = 2.3 Hz, 2H), 3.47 – 3.31 (m, 2H), 3.08 – 2.90 (m, 3H), 2.62 – 2.52 (m, 1H), 2.50 (s, 3H), 2.42 (s, 3H), 2.36 (s, 6H). LRMS (ESI(+)) calcd for $C_{27}H_{31}FN_4O$ $(M+H)^+$ 447.56, found 447.1.

Table 1, Entry 7

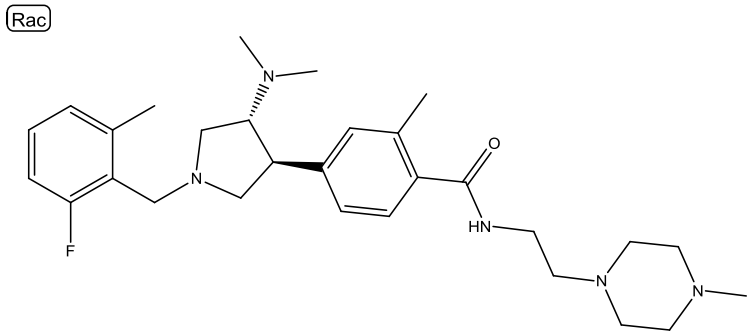

^{1}H NMR (400 MHz, Pyridine-d_5) δ 7.96 (s, 1H), 7.51 – 7.48 (m, 1H), 7.28 – 7.24 (m, 1H), 7.20 – 7.16 (m, 1H), 7.13 – 7.08 (m, 1H), 6.98 – 6.89 (m, 2H), 3.75 – 3.64 (m, 4H), 3.61 – 3.44 (m, 2H), 3.11 (t, *J* = 8.5 Hz, 1H), 3.04 (d, *J* = 6.2 Hz, 2H), 2.85 – 2.76 (m, 9H), 2.75 – 2.71 (m, 2H), 2.58 (dd, *J* = 9.1, 6.0 Hz, 1H), 2.49 – 2.43 (m, 9H), 2.43 – 2.38 (m, 5H). LRMS (ESI(+)) calcd for $C_{29}H_{42}FN_4O(M+H)^+$ 496.34, found 496.1.

Table 1, Entry 8

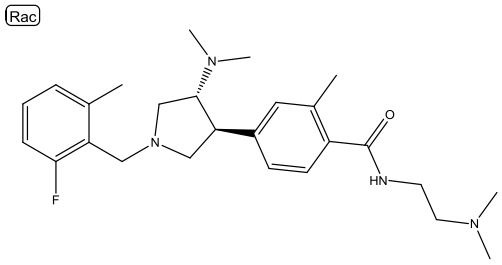

^{1}H NMR (400 MHz, Pyridine-d_5) δ 8.15 (s, 1H), 7.26 (s, 1H), 7.22 – 7.17 (m, 1H), 7.13 – 7.07 (m, 2H), 6.99 – 6.87 (m, 2H), 3.83 – 3.74 (m, 2H), 3.71 – 3.64 (m, 2H), 3.47 – 3.37 (m, 2H), 3.13 – 2.98 (m, 2H), 2.98 –

2.89 (m, 3H), 2.64 – 2.56 (m, 1H), 2.54 (s, 3H), 2.51 – 2.46 (m, 6H), 2.43 (s, 3H), 2.37 (s, 6H). LRMS (ESI(+)) calcd for $C_{26}H_{34}FN_4O$ $(M+H)^+$ 441.60, found 441.1.

Table 1, Entry 9

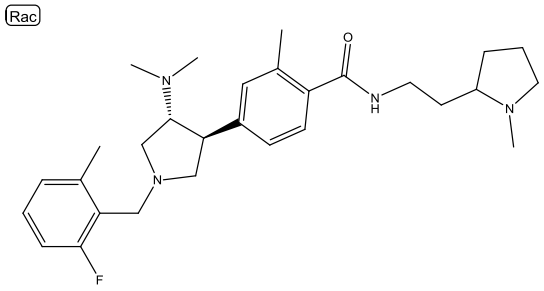

^{1}H NMR (400 MHz, Pyridine-d_5) δ 8.25 (s, 1H), 7.28 – 7.23 (m, 1H), 7.21 – 7.15 (m, 2H), 7.13 – 7.08 (m, 1H), 7.00 – 6.89 (m, 2H), 3.69 (d, *J* = 2.3 Hz, 3H), 3.65 – 3.56 (m, 1H), 3.53 – 3.43 (m, 1H), 3.43 – 3.30 (m, 2H), 3.11 – 2.94 (m, 3H), 2.94 – 2.86 (m, 1H), 2.71 – 2.57 (m, 5H), 2.54 (s, 3H), 2.42-2.40 (m, 2H), 2.37 – 2.26 (m, 7H), 2.23 – 2.12 (m, 1H), 2.12 – 1.99 (m, 1H), 1.91 – 1.68 (m, 3H). LRMS (ESI(+)) calcd for $C_{29}H_{41}FN_4O$ $(M+H)^+$ 481.33, found 481.1.

Table 1, Entry 10

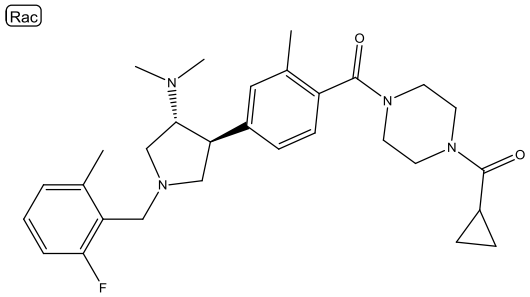

^{1}H NMR (400 MHz, Pyridine-d_5) δ 7.37 – 7.32 (m, 1H), 7.30 – 7.20 (m, 2H), 7.13 – 7.07 (m, 1H), 7.02 – 6.87 (m, 3H), 3.71 (d, *J* = 2.3 Hz, 2H), 3.59 – 3.51 (m, 3H), 3.51 – 3.43 (m, 2H), 3.18 – 3.08 (m, 1H), 3.08 – 2.95 (m, 3H), 2.76 (s, 1H), 2.70 – 2.60 (m, 1H), 2.49 – 2.44 (m, 8H), 2.44 – 2.39 (m, 5H), 2.34 (s, 3H), 1.82 – 1.70 (m, 1H), 1.09 – 0.98 (m, 2H), 0.69 (dq, *J* = 8.2, 3.5 Hz, 2H). LRMS (ESI(+)) calcd for $C_{30}H_{39}FN_4O_2$ $(M+H)^+$ 508.31, found 508.1.

Table 1, Entry 11

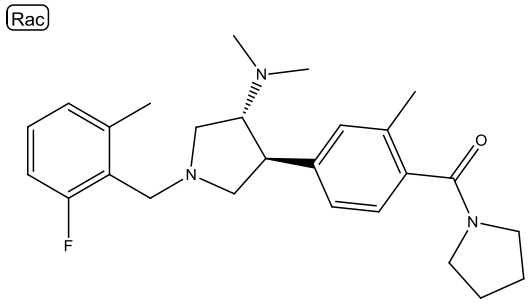

^{1}H NMR (400 MHz, Pyridine-d_5) δ 7.31 (s, 1H), 7.26 – 7.23 (m, 2H), 7.12 – 7.07 (m, 1H), 6.99 – 6.87 (m, 2H), 3.70 (d, *J* = 2.3 Hz, 2H), 3.66 – 3.53 (m, 1H), 3.50 – 3.41 (m, 2H), 3.16 – 3.07 (m, 2H), 3.04 – 2.93 (m, 3H), 2.64 (dd, *J* = 9.3, 5.4 Hz, 1H), 2.43 (s, 3H), 2.42 (s, 1H), 2.40 – 2.36 (m, 6H), 2.35 (s, 3H), 1.66 (s, 4H). LRMS (ESI(+)) calcd for $C_{26}H_{34}FN_3O$ $(M+H)^+$ 424.57, found 424.1.

Table 1, Entry 12

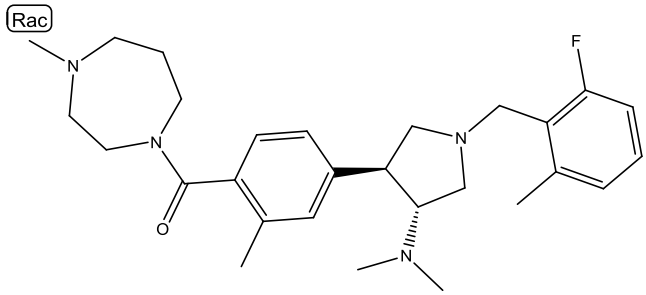

^{1}H NMR (400 MHz, Pyridine-d_5) δ 7.32 (s, 1H), 7.27 – 7.22 (m, 2H), 7.13 – 7.05 (m, 1H), 6.99 – 6.85 (m, 2H), 4.05 – 3.73 (m, 2H), 3.70 (d, *J* = 2.3 Hz, 3H), 3.55 – 3.42 (m, 3H), 3.41 – 3.17 (m, 1H), 3.11 (t, *J* = 8.1 Hz, 1H), 3.05 – 2.93 (m, 3H), 2.75 – 2.69 (m, 3H), 2.67 – 2.57 (m, 2H), 2.42 (s, 2H), 2.41 – 2.38 (m, 7H), 2.34 (s, 4H), 1.91 – 1.67 (m, 2H). LRMS (ESI(+)) calcd for $C_{28}H_{39}FN_4O$ $(M+H)^+$ 467.63, found 467.1.

Table 1, Entry 13

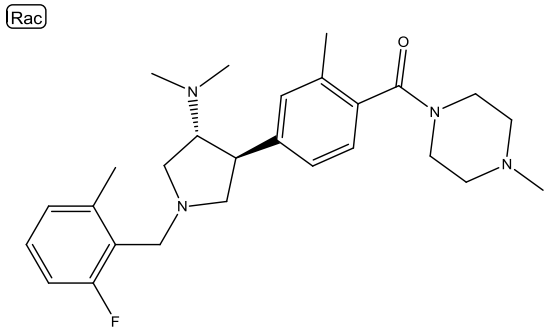

^{1}H NMR (400 MHz, Pyridine-d_5) δ 7.32 (s, 1H), 7.29 – 7.19 (m, 2H), 7.13 – 7.05 (m, 1H), 6.99 – 6.86 (m, 2H), 3.70 (d, *J* = 2.2 Hz, 2H), 3.67 – 3.48 (m, 5H), 3.15 (t, *J* = 8.5 Hz, 1H), 3.10 – 3.00 (m, 2H), 2.70 – 2.57

(m, 2H), 2.53 – 2.44 (m, 7H), 2.40 – 2.28 (m, 8H), 2.22 (d, *J* = 1.1 Hz, 4H). LRMS (ESI(+)) calcd for $C_{27}H_{37}FN_4O$ $(M+H)^+$ 453.61, found 453.1.

Table 1, Entry 14

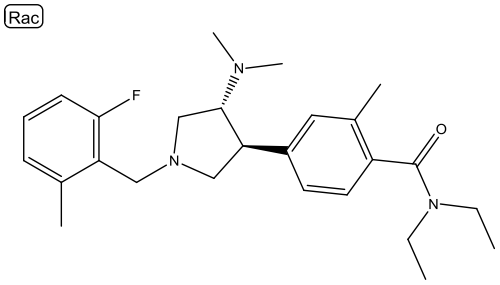

^{1}H NMR (400 MHz, Pyridine-d_5) δ 7.32 – 7.27 (m, 1H), 7.27 – 7.17 (m, 2H), 7.13 – 7.06 (m, 1H), 7.00 – 6.86 (m, 2H), 3.70 (d, *J* = 2.3 Hz, 2H), 3.61 – 3.53 (m, 2H), 3.52 – 3.44 (m, 2H), 3.13 (t, *J* = 8.5 Hz, 2H), 3.03 (d, *J* = 6.3 Hz, 2H), 2.66 – 2.59 (m, 1H), 2.50 – 2.45 (m, 7H), 2.41 (s, 3H), 2.32 (s, 3H), 1.34 – 0.79 (m, 7H). LRMS (ESI(+)) calcd for $C_{26}H_{36}FN_3O$ $(M+H)^+$ 426.58, found 426.2.

Table 1, Entry 15

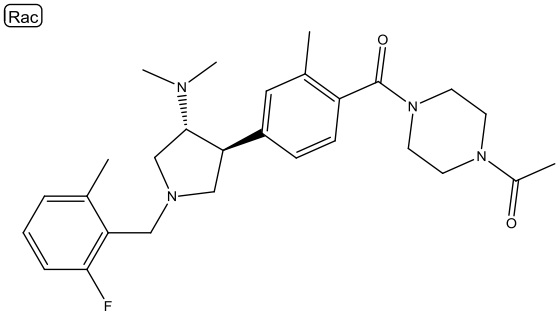

^{1}H NMR (400 MHz, Pyridine-d_5) δ 7.33 (s, 1H), 7.31 – 7.19 (m, 2H), 7.13 – 7.06 (m, 1H), 7.00 – 6.88 (m, 2H), 3.70 (d, *J* = 2.3 Hz, 2H), 3.60 – 3.34 (m, 9H), 3.13 (t, *J* = 8.2 Hz, 1H), 3.02 (d, *J* = 5.9 Hz, 2H), 2.67 – 2.60 (m, 1H), 2.46 – 2.40 (m, 10H), 2.33 (s, 3H), 2.02 (s, 3H). LRMS (ESI(+)) calcd for $C_{28}H_{37}FN_4O_2$ $(M+H)^+$ 481.63, found 481.1.

Table 1, Entry 16

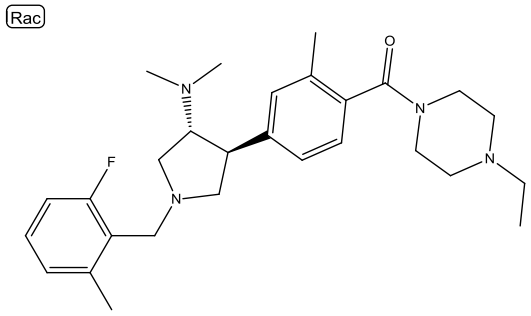

^{1}H NMR (400 MHz, Pyridine-d_5) δ 7.32 (s, 1H), 7.29 – 7.21 (m, 2H), 7.13 – 7.07 (m, 1H), 6.99 – 6.85 (m, 2H), 3.70 (d, *J* = 2.3 Hz, 2H), 3.62 – 3.50 (m, 4H), 3.18 – 3.10 (m, 1H), 3.07 – 3.02 (m, 2H), 2.66 – 2.61 (m, 1H), 2.49 – 2.45 (m, 7H), 2.44 – 2.41 (m, 6H), 2.41 – 2.35 (m, 4H), 2.34 (s, 3H), 1.00 (t, *J* = 7.2 Hz, 3H). LRMS (ESI(+)) calcd for $C_{28}H_{39}FN_4O$ $(M+H)^+$ 467.63, found 467.1.

Table 1, Entry 17

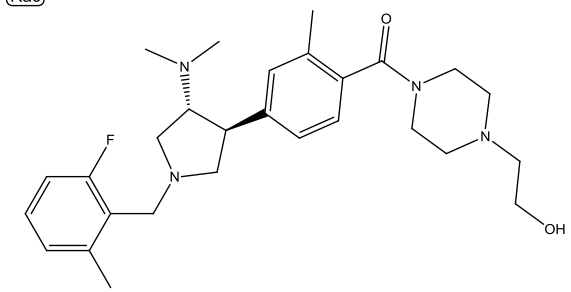

^{1}H NMR (400 MHz, Pyridine-d_5) δ 7.32 (s, 1H), 7.29 – 7.21 (m, 2H), 7.13 – 7.06 (m, 1H), 6.97 – 6.87 (m, 2H), 3.86 (t, *J* = 5.7 Hz, 2H), 3.72 – 3.68 (m, 2H), 3.66 – 3.50 (m, 4H), 3.15 (t, *J* = 8.5 Hz, 1H), 3.11 – 3.01 (m, 2H), 2.71 – 2.65 (m, 3H), 2.65 – 2.60 (m, 2H), 2.57 (s, 4H), 2.51 – 2.48 (m, 6H), 2.42 (s, 3H), 2.34 (s, 3H). LRMS (ESI(+)) calcd for $C_{28}H_{38}FN_4O_2$ $(M+H)^+$ 483.63, found 483.1.

Table 1, Entry 18

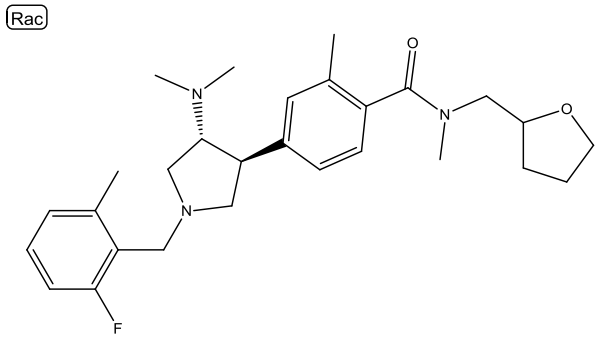

^{1}H NMR (400 MHz, Pyridine-d_5) δ 7.30 (s, 1H), 7.27 – 7.20 (m, 2H), 7.12 – 7.05 (m, 1H), 6.99 – 6.87 (m, 2H), 3.73 – 3.66 (m, 3H), 3.67 – 3.57 (m, 1H), 3.49 – 3.35 (m, 3H), 3.16 – 3.03 (m, 2H), 3.03 – 2.87 (m,

4H), 2.67 – 2.58 (m, 1H), 2.43 (s, 4H), 2.40 – 2.32 (m, 9H), 1.90 – 1.34 (m, 4H). LRMS (ESI(+)) calcd for $C_{28}H_{38}FN_3O_2$ $(M+H)^+$ 468.62, found 468.1.

Table 1, Entry 19

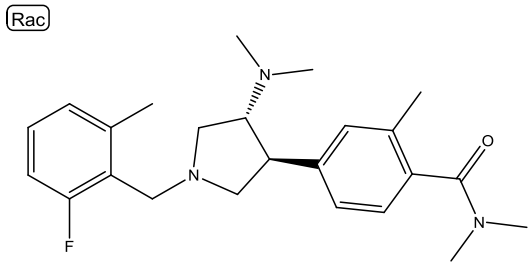

^{1}H NMR (400 MHz, Pyridine-d_5) δ 7.29 (s, 1H), 7.27 – 7.16 (m, 2H), 7.12 – 7.06 (m, 1H), 6.99 – 6.87 (m, 2H), 3.69 (d, *J* = 2.4 Hz, 2H), 3.46 – 3.37 (m, 2H), 3.17 – 3.05 (m, 2H), 3.03 – 2.90 (m, 4H), 2.67 – 2.57 (m, 2H), 2.43 (s, 3H), 2.37 – 2.32 (m, 7H), 2.29 (s, 4H). LRMS (ESI(+)) calcd for $C_{24}H_{32}FN_3O$ $(M+H)^+$ 398.53, found 398.1.

Table 2, Entry 1

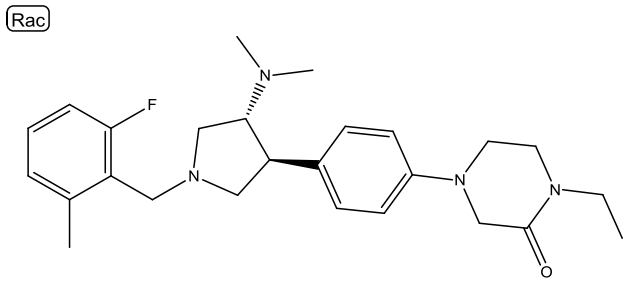

^{1}H NMR (400 MHz, Pyridine-d_5) δ 7.56 – 7.39 (m, 1H), 7.38 – 7.31 (m, 2H), 7.19 – 7.11 (m, 1H), 7.04 – 6.95 (m, 3H), 4.03 (s, 1H), 3.93 – 3.84 (m, 1H), 3.74 – 3.58 (m, 4H), 3.56 – 3.42 (m, 2H), 3.42 – 3.37 (m, 1H), 3.35 – 3.25 (m, 2H), 3.16 (t, *J* = 8.5 Hz, 1H), 3.12 – 3.02 (m, 1H), 2.73 (s, 6H), 2.69 – 2.62 (m, 2H), 2.50 (s, 3H), 2.45 – 2.35 (m, 2H), 1.14 – 0.98 (m, 2H). LRMS (ESI(+)) calcd for $C_{26}H_{35}FN_4O$ $(M+H)^+$ 439.58, found 439.1.

Table 2, Entry 2

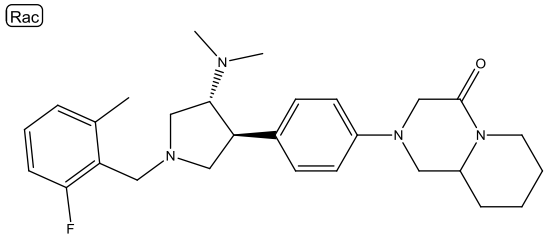

^{1}H NMR (400 MHz, Pyridine-d_5) δ 7.40 – 7.33 (m, 2H), 7.20 – 7.12 (m, 1H), 7.07 – 6.95 (m, 4H), 4.88 (d, *J* = 12.6 Hz, 1H), 4.21 – 4.09 (m, 1H), 3.95 – 3.84 (m, 2H), 3.77 – 3.56 (m, 5H), 3.37 – 3.24 (m, 2H), 3.21 – 3.02 (m, 3H), 3.02 – 2.93 (m, 1H), 2.72 (s, 6H), 2.41 (s, 3H), 1.68 – 1.43 (m, 3H), 1.32 – 1.14 (m, 3H). LRMS (ESI(+)) calcd for $C_{28}H_{37}FN_4O$ $(M+H)^+$ 465.62, found 465.1.

Table 2, Entry 3

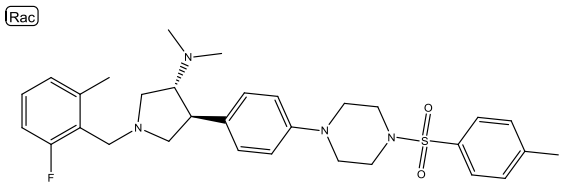

^{1}H NMR (400 MHz, Pyridine-d_5) δ 7.89 – 7.84 (m, 2H), 7.35 – 7.29 (m, 4H), 7.20 – 7.13 (m, 1H), 7.04 – 6.93 (m, 4H), 3.83 – 3.73 (m, 1H), 3.70 – 3.55 (m, 3H), 3.28 – 3.18 (m, 9H), 3.16 – 2.99 (m, 2H), 2.64 (s, 6H), 2.56 – 2.42 (m, 4H), 2.28 (s, 3H). LRMS (ESI(+)) calcd for $C_{31}H_{39}FN_4O_2S$ $(M+H)^+$ 551.73, found 551.1.

Table 2, Entry 4

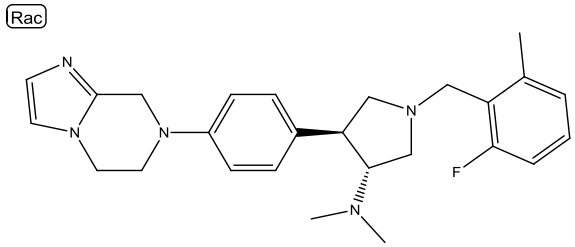

^{1}H NMR (400 MHz, Pyridine-d_5) δ 7.41 – 7.29 (m, 3H), 7.11 – 7.04 (m, 3H), 7.04 – 6.95 (m, 2H), 4.67 (s, 2H), 4.01 (t, *J* = 5.4 Hz, 2H), 3.97 – 3.89 (m, 1H), 3.73 – 3.60 (m, 3H), 3.60 – 3.51 (m, 2H), 3.22 – 3.02 (m, 2H), 2.75 (s, 6H), 2.50 (s, 2H), 2.40 (s, 3H). LRMS (ESI(+)) calcd for $C_{26}H_{32}FN_5$ $(M+H)^+$ 434.56, found 434.1.

Table 2, Entry 5

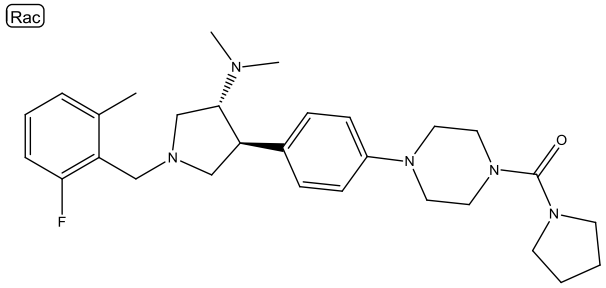

^{1}H NMR (400 MHz, Pyridine-d_5) δ 7.39 – 7.28 (m, 2H), 7.19 – 7.13 (m, 1H), 7.06 – 6.95 (m, 4H), 3.97 – 3.89 (m, 1H), 3.74 – 3.57 (m, 4H), 3.52 – 3.45 (m, 4H), 3.43 – 3.35 (m, 4H), 3.35 – 3.28 (m, 1H), 3.24 – 3.14 (m, 5H), 3.13 – 3.05 (m, 1H), 2.75 (s, 6H), 2.40 (s, 3H), 1.65 – 1.55 (m, 4H). LRMS (ESI(+)) calcd for $C_{29}H_{40}FN_5O$ $(M+H)^+$ 494.66, found 494.1.

Table 2, Entry 6

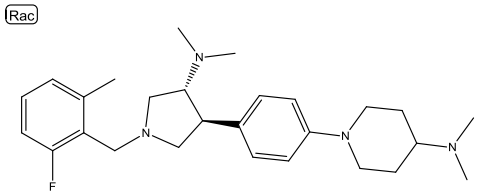

^{1}H NMR (400 MHz, Pyridine-d_5) δ 7.38 – 7.31 (m, 2H), 7.19 – 7.14 (m, 1H), 7.04 – 6.94 (m, 4H), 3.97 – 3.87 (m, 1H), 3.82 – 3.56 (m, 5H), 3.36 – 3.21 (m, 2H), 3.16 (t, *J* = 8.5 Hz, 1H), 3.12 – 3.04 (m, 1H), 2.79 (s, 6H), 2.74 (s, 6H), 2.62 (t, *J* = 12.0 Hz, 2H), 2.40 (s, 3H), 2.18 – 2.08 (m, 2H), 1.92 – 1.78 (m, 2H). LRMS (ESI(+)) calcd for $C_{27}H_{39}FN_4O$ $(M+H)^+$ 439.62, found 439.2.

Table 2, Entry 7

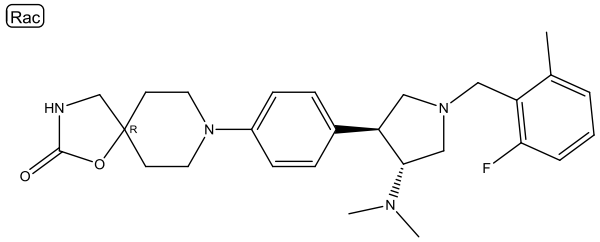

^{1}H NMR (400 MHz, Pyridine-d_5) δ 7.77 – 7.70 (m, 2H), 7.52 – 7.46 (m, 2H), 7.20 – 7.14 (m, 1H), 7.05 – 6.97 (m, 2H), 3.92 – 3.81 (m, 3H), 3.76 – 3.60 (m, 5H), 3.52 – 3.40 (m, 2H), 3.28 – 3.21 (m, 1H), 3.21 – 3.16 (m, 1H), 3.16 – 3.08 (m, 1H), 2.84 (s, 1H), 2.70 (s, 6H), 2.62 – 2.51 (m, 3H), 2.51 – 2.48 (m, 1H), 2.25 – 2.16 (m, 2H), 1.98 (s, 1H). LRMS (ESI(+)) calcd for $C_{27}H_{34}FN_4O_2$ $(M+H)^+$ 467.58, found 467.1.

Table 2, Entry 8

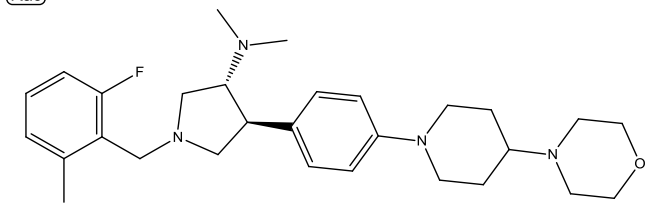

^{1}H NMR (400 MHz, Pyridine-d_5) δ 7.38 – 7.31 (m, 2H), 7.20 – 7.13 (m, 1H), 7.05 – 6.95 (m, 4H), 4.03 – 3.90 (m, 1H), 3.89 – 3.83 (m, 4H), 3.80 – 3.70 (m, 2H), 3.70 – 3.57 (m, 3H), 3.33 (dd, *J* = 10.6, 4.2 Hz, 1H), 3.17 (t, *J* = 8.5 Hz, 1H), 3.09 (dd, *J* = 10.7, 7.5 Hz, 1H), 2.84 (s, 1H), 2.80 – 2.76 (m, 3H), 2.75 (s, 6H), 2.68 (s, 2H), 2.66 – 2.55 (m, 3H), 2.51 (d, *J* = 7.5 Hz, 1H), 1.97 (s, 3H), 1.80 – 1.66 (m, 2H). LRMS (ESI(+)) calcd for $C_{29}H_{41}FN_4O$ $(M+H)^+$ 481.66, found 481.1.

Table 2, Entry 9

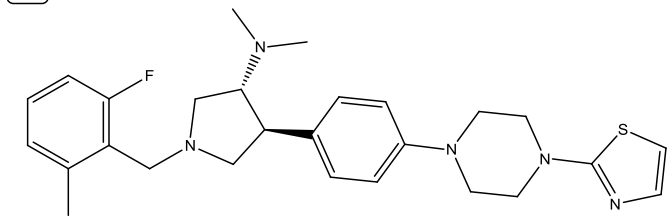

^{1}H NMR (400 MHz, Pyridine-d_5) δ 7.46 (d, *J* = 3.6 Hz, 1H), 7.40 – 7.30 (m, 2H), 7.20 – 7.13 (m, 1H), 7.04 – 6.98 (m, 4H), 6.82 (d, *J* = 3.6 Hz, 1H), 3.96 (dt, *J* = 7.3, 4.6 Hz, 1H), 3.75 – 3.67 (m, 1H), 3.66 – 3.61 (m, 5H), 3.34 (dd, *J* = 10.7, 4.2 Hz, 1H), 3.27 – 3.21 (m, 4H), 3.18 (t, *J* = 8.5 Hz, 1H), 3.10 (dd, *J* = 10.6, 7.6 Hz, 1H), 2.77 (s, 6H), 2.55 – 2.46 (m, 2H), 2.40 (s, 3H). LRMS (ESI(+)) calcd for $C_{27}H_{34}FN_5S$ $(M+H)^+$ 480.66, found 480.1.

Table 2, Entry 10

Rac

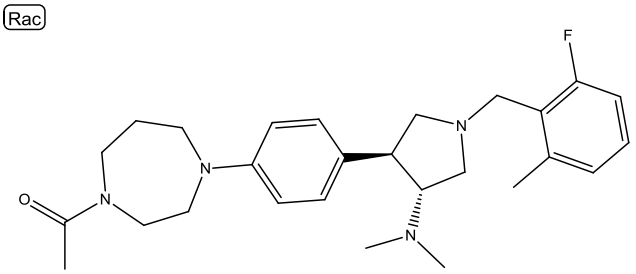

^{1}H NMR (400 MHz, Pyridine-d_5) δ 7.34 – 7.26 (m, 2H), 7.19 – 7.12 (m, 1H), 7.03 – 6.94 (m, 2H), 6.82 – 6.75 (m, 2H), 3.95 – 3.87 (m, 1H), 3.81 – 3.74 (m, 1H), 3.70 – 3.51 (m, 5H), 3.50 – 3.38 (m, 4H), 3.35 – 3.28 (m, 1H), 3.20 – 3.10 (m, 2H), 3.10 – 3.01 (m, 1H), 2.73 (s, 6H), 2.54 – 2.45 (m, 2H), 2.39 (s, 3H), 2.01 (s, 2H), 1.94 (s, 2H), 1.84 – 1.75 (m, 1H). LRMS (ESI(+)) calcd for $C_{27}H_{37}FN_4O$ $(M+H)^+$ 453.61, found 453.1.

Table 2, Entry 11

Rac

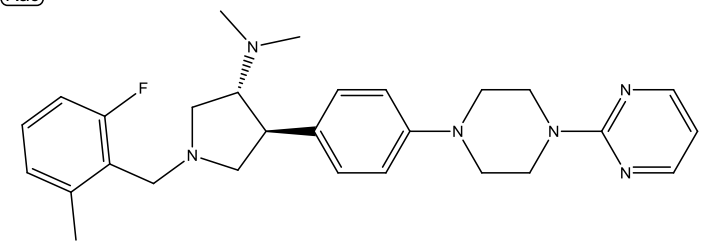

^{1}H NMR (400 MHz, Pyridine-d_5) δ 8.44 (d, J = 4.7 Hz, 2H), 7.39 – 7.32 (m, 2H), 7.19 – 7.13 (m, 1H), 7.07 – 6.95 (m, 4H), 6.51 (t, J = 4.7 Hz, 1H), 4.10 – 4.01 (m, 4H), 3.96 – 3.88 (m, 1H), 3.72 – 3.57 (m, 3H), 3.36 – 3.28 (m, 1H), 3.25 – 3.19 (m, 4H), 3.19 – 3.04 (m, 2H), 2.74 (s, 6H), 2.57 – 2.51 (m, 1H), 2.40 (s, 3H). LRMS (ESI(+)) calcd for $C_{28}H_{35}FN_6$ $(M+H)^+$ 475.62, found 475.1.

Table 2, Entry 12

Rac

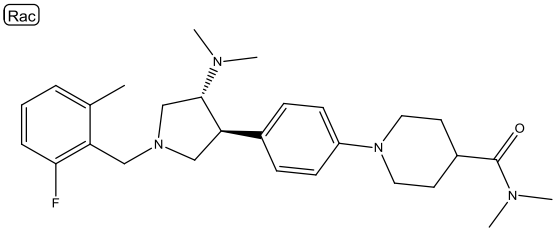

^{1}H NMR (400 MHz, Pyridine-d_5) δ 7.35 – 7.28 (m, 2H), 7.19 – 7.12 (m, 1H), 7.06 – 6.94 (m, 4H), 3.88 (dt, J = 7.3, 4.7 Hz, 1H), 3.82 – 3.72 (m, 2H), 3.72 – 3.60 (m, 3H), 3.36 – 3.26 (m, 1H), 3.15 (t, J = 8.5 Hz, 1H), 3.11 – 3.03 (m, 1H), 2.94 – 2.89 (m, 6H), 2.75 – 2.65 (m, 9H), 2.41 (s, 3H), 2.17 – 2.03 (m, 2H), 1.89 – 1.78 (m, 2H). LRMS (ESI(+)) calcd for $C_{28}H_{39}FN_4O$ $(M+H)^+$ 467.63, found 467.1.

Table 2, Entry 13

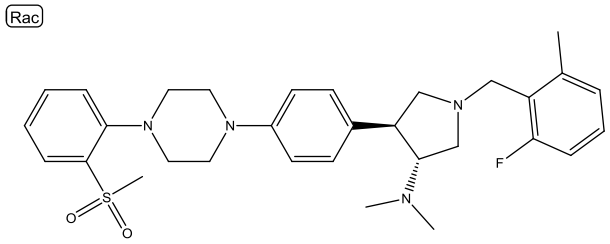

^{1}H NMR (400 MHz, Pyridine-d_5) δ 8.32 (dd, *J* = 7.9, 1.6 Hz, 1H), 7.65 – 7.59 (m, 1H), 7.49 – 7.42 (m, 1H), 7.42 – 7.36 (m, 2H), 7.36 – 7.29 (m, 1H), 7.20 – 7.14 (m, 1H), 7.08 – 6.97 (m, 4H), 3.98 – 3.91 (m, 1H), 3.74 – 3.68 (m, 1H), 3.63 (td, *J* = 12.4, 11.7, 2.2 Hz, 2H), 3.51 (s, 3H), 3.42 – 3.30 (m, 5H), 3.27 – 3.14 (m, 5H), 3.14 – 3.06 (m, 1H), 2.76 (s, 6H), 2.59 – 2.51 (m, 1H), 2.42 (s, 3H). LRMS (ESI(+)) calcd for $C_{31}H_{34}FN_4O_2S$ $(M+H)^+$ 551.73, found 551.1.

Table 2, Entry 14

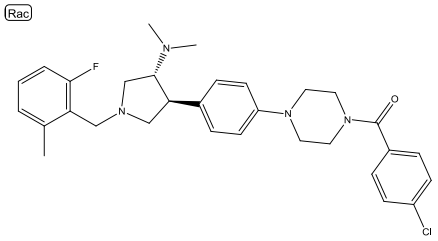

^{1}H NMR (400 MHz, Pyridine-d_5) δ 7.57 – 7.55 (m, 2H), 7.50 – 7.44 (m, 2H), 7.40 – 7.33 (m, 2H), 7.20 – 7.14 (m, 1H), 7.06 – 6.96 (m, 4H), 3.89 – 3.75 (m, 2H), 3.73 – 3.52 (m, 5H), 3.27 (dd, *J* = 10.6, 4.4 Hz, 2H), 3.22 – 3.10 (m, 5H), 3.07 (dd, *J* = 10.5, 7.5 Hz, 1H), 2.68 (s, 6H), 2.57 – 2.48 (m, 2H), 2.41 (s, 3H). LRMS (ESI(+)) calcd for $C_{31}H_{36}ClFN_4O$ $(M+H)^+$ 535.10, found 535.0.

Table 2, Entry 15

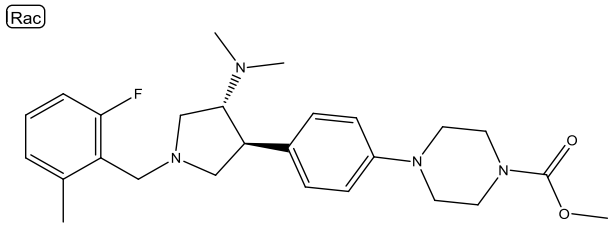

^{1}H NMR (400 MHz, Pyridine-d_5) δ 7.38 – 7.32 (m, 2H), 7.19 – 7.13 (m, 1H), 7.04 – 6.96 (m, 4H), 3.83 – 3.76 (m, 1H), 3.72 (s, 3H), 3.68 – 3.54 (m, 7H), 3.24 (dd, *J* = 10.4, 4.5 Hz, 1H), 3.19 – 3.11 (m, 1H), 3.11 – 3.04 (m, 4H), 2.65 (s, 6H), 2.59 – 2.47 (m, 2H), 2.44 – 2.36 (m, 3H). LRMS (ESI(+)) calcd for $C_{26}H_{35}FN_4O_2$ $(M+H)^+$ 455.58, found 455.1.

Table 2, Entry 16

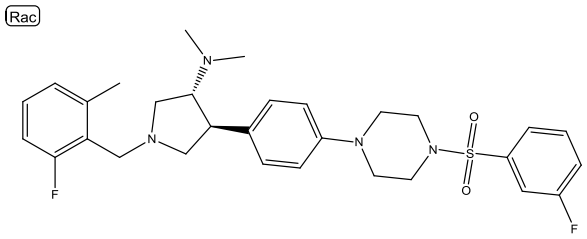

^{1}H NMR (400 MHz, Pyridine-d_5) δ 7.82 (ddd, *J* = 8.3, 2.6, 1.6 Hz, 1H), 7.79 – 7.72 (m, 1H), 7.56 – 7.52 (m, 1H), 7.41 (tdd, *J* = 8.5, 2.6, 1.0 Hz, 1H), 7.36 – 7.31 (m, 2H), 7.19 – 7.14 (m, 1H), 7.04 – 6.95 (m, 4H), 3.77 – 3.68 (m, 1H), 3.68 – 3.53 (m, 3H), 3.23 – 3.19 (m, 8H), 3.11 (t, *J* = 8.5 Hz, 1H), 3.03 (dd, *J* = 10.3, 7.5 Hz, 1H), 2.59 (s, 6H), 2.54 – 2.45 (m, 2H), 2.40 (s, 3H). LRMS (ESI(+)) calcd for $C_{30}H_{36}F_2N_4O_2$ $(M+H)^{+}$ 555.69, found 555.0.

Table 2, Entry 17

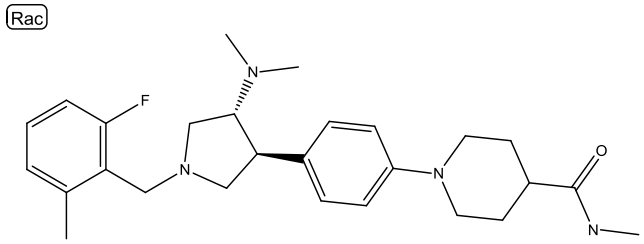

^{1}H NMR (400 MHz, Pyridine-d_5) δ 7.34 – 7.28 (m, 2H), 7.19 – 7.13 (m, 1H), 7.03 – 6.94 (m, 4H), 3.79 – 3.69 (m, 2H), 3.69 – 3.57 (m, 3H), 3.33 (dd, *J* = 10.6, 4.2 Hz, 1H), 3.16 (t, *J* = 8.5 Hz, 1H), 3.08 (dd, *J* = 10.6, 7.6 Hz, 1H), 2.93 (d, *J* = 4.6 Hz, 3H), 2.75 (s, 6H), 2.70 – 2.61 (m, 2H), 2.54 – 2.44 (m, 2H), 2.40 (s, 3H), 2.20 – 2.05 (m, 2H), 2.04 – 1.96 (m, 2H). LRMS (ESI(+)) calcd for $C_{27}H_{36}FN_4O$ $(M+H)^{+}$ 453.62, found 453.1.

Table 2, Entry 18

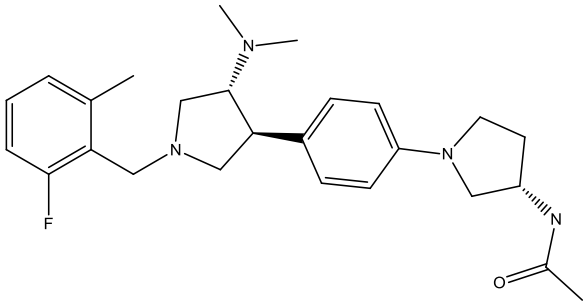

^{1}H NMR (400 MHz, Pyridine-d_5) δ 7.20 – 7.13 (m, 1H), 7.05 – 6.94 (m, 3H), 6.53 – 6.46 (m, 3H), 4.85 – 4.75 (m, 1H), 3.98 – 3.91 (m, 1H), 3.71 – 3.56 (m, 4H), 3.41 – 3.32 (m, 1H), 3.32 – 3.25 (m, 2H), 3.21 – 3.12 (m, 2H), 3.08 (dd, *J* = 10.7, 7.6 Hz, 1H), 2.78 (s, 6H), 2.53 – 2.46 (m, 1H), 2.40 (s, 3H), 2.25 – 2.11 (m, 1H), 2.10 – 1.96 (m, 4H). LRMS (ESI(+)) calcd for $C_{26}H_{34}FN_4O$ $(M+H)^{+}$ 439.59, found 439.1.

Table 2, Entry 19

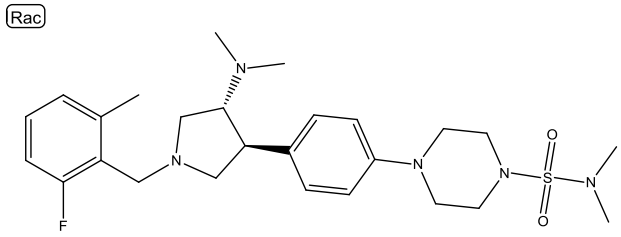

^{1}H NMR (400 MHz, Pyridine-d_5) δ 7.39 – 7.33 (m, 2H), 7.20 – 7.14 (m, 1H), 7.06 – 6.96 (m, 4H), 3.98 – 3.90 (m, 1H), 3.73 – 3.58 (m, 3H), 3.50 – 3.43 (m, 4H), 3.36 – 3.29 (m, 1H), 3.25 – 3.18 (m, 4H), 3.18 – 3.13 (m, 1H), 3.13 – 3.05 (m, 1H), 2.83 (s, 6H), 2.75 (s, 6H), 2.55 – 2.48 (m, 1H), 2.40 (s, 3H). LRMS (ESI(+)) calcd for $C_{26}H_{35}FN_5O_2S$ $(M+H)^+$ 504.68, found 504.1.

Table 2, Entry 20

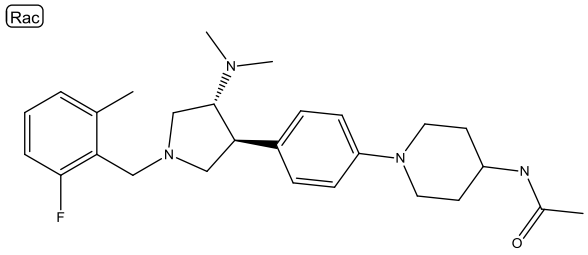

^{1}H NMR (400 MHz, Pyridine-d_5) δ 7.39 – 7.27 (m, 2H), 7.19 – 7.14 (m, 1H), 7.02 – 6.94 (m, 4H), 4.27 – 4.13 (m, 1H), 3.99 – 3.91 (m, 1H), 3.72 – 3.55 (m, 5H), 3.38 – 3.31 (m, 1H), 3.15 (t, *J* = 8.5 Hz, 1H), 3.12 – 3.02 (m, 1H), 2.80 – 2.72 (m, 7H), 2.52 – 2.44 (m, 1H), 2.39 (s, 3H), 2.14 – 2.03 (m, 5H), 1.78 – 1.61 (m, 2H). LRMS (ESI(+)) calcd for $C_{27}H_{36}FN_4O$ $(M+H)^+$ 453.62, found 453.1.

Table 2, Entry 21

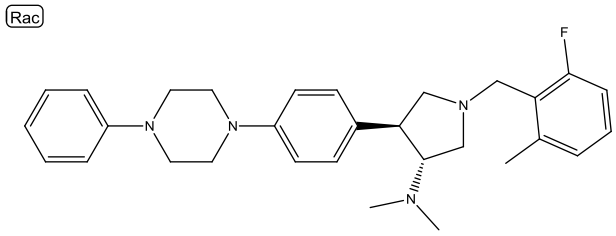

^{1}H NMR (400 MHz, Pyridine-d_5) δ 7.41 – 7.33 (m, 4H), 7.20 – 7.14 (m, 1H), 7.12 – 6.93 (m, 7H), 4.00 – 3.91 (m, 1H), 3.75 – 3.67 (m, 1H), 3.67 – 3.57 (m, 2H), 3.39 – 3.32 (m, 1H), 3.32 – 3.25 (m, 8H), 3.18 (t, *J* = 8.5 Hz, 1H), 3.10 (dd, *J* = 10.7, 7.6 Hz, 1H), 2.76 (s, 6H), 2.57 – 2.48 (m, 1H), 2.41 (s, 3H). LRMS (ESI(+)) calcd for $C_{30}H_{37}FN_4O$ $(M+H)^+$ 473.65, found 473.1.

Table 2, Entry 22

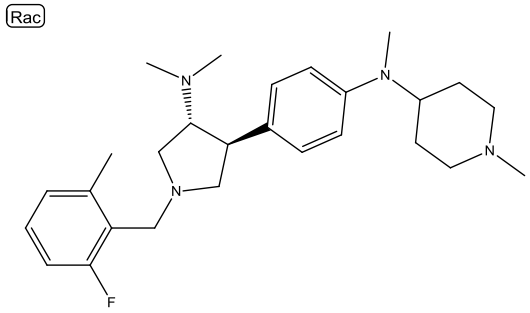

^{1}H NMR (400 MHz, Pyridine-d_5) δ 7.35 – 7.27 (m, 2H), 7.19 – 7.13 (m, 1H), 7.03 – 6.96 (m, 4H), 4.01 – 3.90 (m, 2H), 3.73 – 3.63 (m, 2H), 3.63 – 3.53 (m, 3H), 3.39 – 3.30 (m, 1H), 3.18 (t, *J* = 8.5 Hz, 1H), 3.08 (dd, *J* = 10.8, 7.6 Hz, 1H), 3.03 – 2.91 (m, 2H), 2.81 – 2.75 (m, 9H), 2.73 (s, 3H), 2.55 – 2.49 (m, 1H), 2.47 – 2.34 (m, 5H), 1.83 – 1.70 (m, 2H). LRMS (ESI(+)) calcd for $C_{27}H_{39}FN_4O$ $(M+H)^+$ 439.63, found 439.1.

Table 2, Entry 23

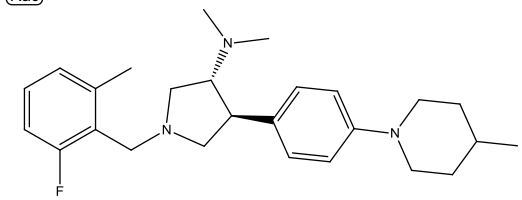

^{1}H NMR (400 MHz, Pyridine-d_5) δ 7.35 – 7.29 (m, 2H), 7.19 – 7.13 (m, 1H), 7.04 – 6.94 (m, 4H), 4.00 – 3.91 (m, 1H), 3.72 – 3.56 (m, 5H), 3.39 – 3.30 (m, 1H), 3.16 (t, *J* = 8.5 Hz, 1H), 3.12 – 3.03 (m, 1H), 2.75 (s, 6H), 2.65 – 2.54 (m, 2H), 2.54 – 2.47 (m, 1H), 2.40 (s, 3H), 1.61 – 1.49 (m, 2H), 1.38 – 1.28 (m, 1H), 1.22 (qd, *J* = 11.8, 3.8 Hz, 2H), 0.85 (d, *J* = 6.2 Hz, 3H). LRMS (ESI(+)) calcd for $C_{27}H_{39}FN_4$ $(M+H)^+$ 410.59, found 410.2.

Table 2, Entry 24

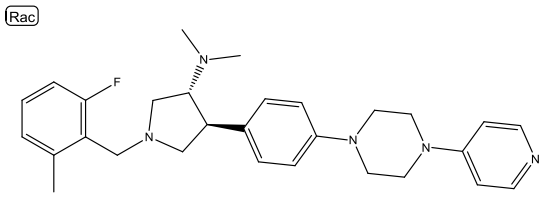

^{1}H NMR (400 MHz, Pyridine-d_5) δ 8.52 – 8.47 (m, 2H), 7.43 – 7.37 (m, 2H), 7.19 – 7.14 (m, 1H), 7.06 – 6.98 (m, 6H), 4.00 – 3.92 (m, 1H), 3.76 – 3.58 (m, 7H), 3.38 – 3.30 (m, 5H), 3.19 (t, *J* = 8.5 Hz, 1H), 3.09 (dd, *J* = 10.7, 7.5 Hz, 1H), 2.76 (s, 6H), 2.58 – 2.49 (m, 1H), 2.41 (s, 3H). LRMS (ESI(+)) calcd for $C_{29}H_{36}FN_5$ $(M+H)^+$ 474.64, found 474.1.

Table 2, Entry 25

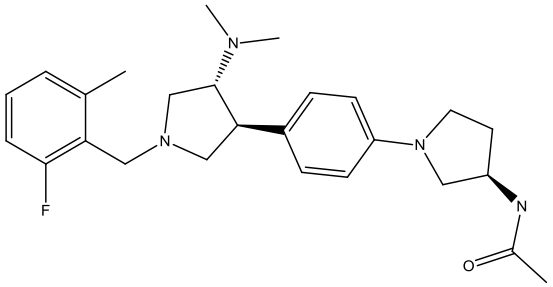

^{1}H NMR (400 MHz, Pyridine-d_5) δ 8.83 – 8.76 (m, 1H), 7.19 – 7.14 (m, 1H), 7.04 – 6.98 (m, 2H), 6.52 – 6.48 (m, 3H), 4.84 – 4.73 (m, 1H), 3.99 – 3.91 (m, 1H), 3.69 – 3.55 (m, 4H), 3.40 – 3.32 (m, 1H), 3.32 – 3.25 (m, 2H), 3.20 – 3.12 (m, 2H), 3.12 – 3.04 (m, 1H), 2.78 (s, 6H), 2.52 – 2.45 (m, 1H), 2.40 (s, 3H), 2.24 – 2.12 (m, 1H), 2.08 (s, 3H), 2.06 – 1.98 (m, 1H). LRMS (ESI(+)) calcd for $C_{26}H_{34}FN_4O$ $(M+H)^+$ 439.59, found 439.1.

Table 2, Entry 26

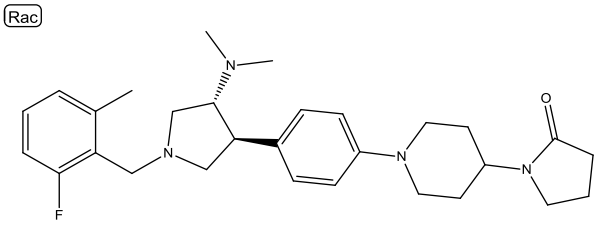

^{1}H NMR (400 MHz, Pyridine-d_5) δ 7.38 – 7.31 (m, 2H), 7.20 – 7.14 (m, 1H), 7.04 – 6.96 (m, 4H), 4.32 – 4.20 (m, 1H), 3.99 – 3.90 (m, 1H), 3.76 – 3.66 (m, 3H), 3.66 – 3.57 (m, 2H), 3.38 – 3.30 (m, 1H), 3.23 – 3.13 (m, 1H), 3.13 – 3.05 (m, 3H), 2.75 (s, 6H), 2.72 – 2.62 (m, 2H), 2.55 – 2.47 (m, 1H), 2.40 (s, 3H), 2.35 – 2.28 (m, 2H), 1.83 – 1.69 (m, 4H), 1.69 – 1.59 (m, 2H). LRMS (ESI(+)) calcd for $C_{29}H_{39}FN_4O$ $(M+H)^+$ 479.66, found 479.1.

Table 2, Entry 27

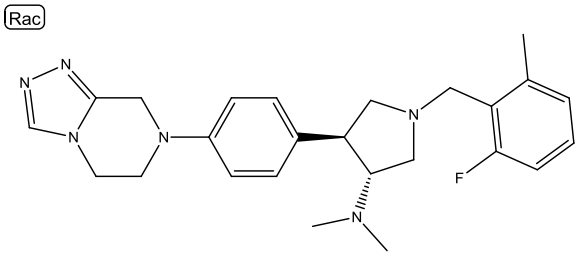

^{1}H NMR (400 MHz, Pyridine-d_5) δ 8.55 (s, 1H), 7.41 – 7.34 (m, 2H), 7.20 – 7.14 (m, 1H), 7.13 – 7.08 (m, 2H), 7.03 – 6.98 (m, 2H), 4.73 (s, 2H), 4.07 (t, J = 5.4 Hz, 2H), 4.00 – 3.92 (m, 1H), 3.75 – 3.67 (m, 1H), 3.67 – 3.58 (m, 4H), 3.36 – 3.29 (m, 1H), 3.18 (t, J = 8.5 Hz, 1H), 3.14 – 3.06 (m, 1H), 2.76 (s, 6H), 2.55 – 2.49 (m, 1H), 2.40 (s, 3H). LRMS (ESI(+)) calcd for $C_{25}H_{31}FN_6$ $(M+H)^+$ 435.56, found 435.1.

Table 2, Entry 28

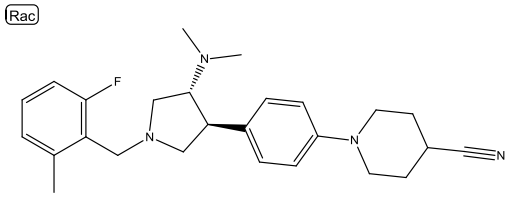

^{1}H NMR (400 MHz, Pyridine-d_5) δ 7.38 – 7.31 (m, 2H), 7.19 – 7.13 (m, 1H), 7.04 – 6.94 (m, 4H), 3.97 – 3.89 (m, 1H), 3.72 – 3.57 (m, 3H), 3.40 – 3.29 (m, 3H), 3.17 (t, *J* = 8.5 Hz, 1H), 3.12 – 3.05 (m, 1H), 3.01 – 2.92 (m, 2H), 2.86 – 2.78 (m, 1H), 2.75 (s, 6H), 2.55 – 2.48 (m, 1H), 2.40 (s, 3H), 1.93 – 1.76 (m, 4H). LRMS (ESI(+)) calcd for $C_{26}H_{33}FN_4$ $(M+H)^+$ 421.58, found 421.1.

Table 2, Entry 29

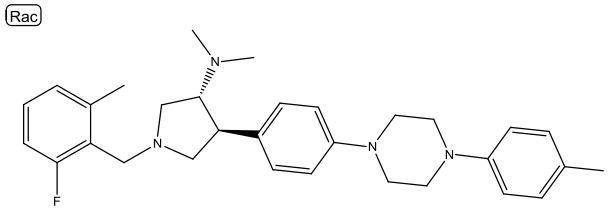

^{1}H NMR (400 MHz, Pyridine-d_5) δ 7.39 – 7.33 (m, 2H), 7.19 – 7.13 (m, 3H), 7.08 – 7.03 (m, 2H), 7.03 – 6.97 (m, 4H), 3.96 – 3.90 (m, 1H), 3.72 – 3.59 (m, 3H), 3.36 – 3.25 (m, 9H), 3.18 (t, *J* = 8.5 Hz, 1H), 3.13 – 3.05 (m, 1H), 2.75 (s, 6H), 2.57 – 2.48 (m, 1H), 2.41 (s, 3H), 2.24 (s, 3H). LRMS (ESI(+)) calcd for $C_{31}H_{39}FN_4$ $(M+H)^+$ 487.68, found 487.1.

References

(1) Chemspeed Technologies. www.chemspeed.com

(2) Tu, N.P.; Sarris K; Searle P.A. `An Automated Microwave Assisted Synthesis-Purification System for Rapid Generation of Compound Libraries.` *JALA*, **2016**, 21 (3), 459-69.

(3) Thermo Scientific. www.thermofisher.com

(4) Neue, U.D.; Mazza, C.B.; Cavanaugh, J.Y.; Lu, Z.; Wheat, T.E. `At-column dilution for improved loading in preparative chromatography.` *Chromatographia,* **2003**, *57*, S121-S127.

(5) Curtin, M.L.; Pliushchev, M.A.; Li, H.Q.; Torrent, M.; Dietrich, J.D.; Jakob, C.G.; Zhu, H.; Zhao, H.; Wang, Y.; Ji ,Z.; Clark, R.F.; Sarris, K.A.; Jagadeeswaran, S.; Shaw, B.; Algire, M.A.; He, Y.; Richardson, P.L.; Sweis, R.S.; Sun, C.; Chiang, G.G.; Michaelides, M.R.; `Amino pyrrolidines as potent and novel protein-protein interaction inhibitors of the PRC2 complex.` *Bioorg. Med Chem. Lett.*, **2017**, 27, 1576.

(6) He, Y.; Selvaraju, S.; Curtin, M. L.; Jakob, C. G.; Zhu, H.; Comess, K. M.; Shaw, B.; Galasinski, S.; The, J.; Lima-Fernandes, E.; Szewczyk, M.; Cheng, D.; Klinge, K. L.; Li, H.-Q.; Pliushchev, M.; Algire, M. A.; Maag, D.; Guo, J.; Panchal, S. C.; Sweis, R. F.; Torrent, M.; Bigelow, L. J.; Senisterra, G.; Li, F.; Kennedy, S.; Wu, Q.; Osterling, D. J.; Lindley, D. J.; Goa, W.; Petros, A. M.; Dietrich, J.; Barsyte-Lovejoy, D.; Vedadi, M.; Buchanan, F. G.; Arrowsmith, C. H.; Chiang, G. G.; Sun, C.; Pappano, W. N.; `The EED protein-protein interaction inhibitor A-395 inactivates the PRC2 complex.` *Nat. Chem. Biol*., **2017**, 13, 389.